A Numerical Study of the Effects of Oxy-Fuel Combustion under Homogeneous Charge Compression Ignition Regime

Raouf Mobasheri [1,2,*], Abdel Aitouche [1,2], Zhijun Peng [3], Xiang Li [3]

[1] Univ. Lille, CNRS, Centrale Lille, UMR 9189 - CRIStAL - Centre de Recherche en Informatique Signal et Automatique de Lille, F-59000 Lille, France.

[2] Junia, Smart Systems and Energies, F-59000 Lille, France.

[3] School of Computer Science and Technology, University of Bedfordshire, Luton, LU1 3JU, United Kingdom.

*Corresponding author: Raouf Mobasheri, raouf.mobasheri@junia.com

Abstract

The European Union (EU) has recently adopted new directives to reduce the level of pollutant emissions from non-road mobile machinery engines. The main scope of project RIVER for which this study is relating is to develop possible solutions to achieve nitrogen-free combustion and zero-carbon emissions in diesel engines. RIVER aims to apply an oxy-fuel combustion with Carbon Capture and Storage (CCS) technology to eliminate NOx emission and to capture and store carbon emissions. As part of this project, a computational fluid dynamic (CFD) analysis has been performed to investigate the effects of oxy-fuel combustion on combustion characteristics and engine operating conditions in a diesel engine under Homogenous Charge Compression Ignition (HCCI) mode. A reduced chemical n-heptane-n-butanol-PAH mechanism which consists of 76 species and 349 reactions has been applied for oxy-fuel HCCI combustion modeling. Different diluent strategies based on the volume fraction of oxygen and a diluent gas has been considered over a wide range of air-fuel equivalence ratios. Variation in the diluent ratio has been achieved by adding different percentages of carbon dioxide for a range from 77 to 83 vol. % in the intake charge. Results show that indicated thermal efficiency (ITE) has reduced from 32.7% to 20.9% as

the CO_2 concentration has increased from 77% to 83% at low engine loads while it doesn't bring any remarkable change at high engine loads. It has also found that this technology has brought CO and PM emissions to very ultra-low level (near zero) while NOx emissions have been completely eliminated.

Keywords

Oxy-fuel, HCCI combustion, Diesel Engine, Diluent Strategies, Pollutant Emissions

1. Introduction

Many new technologies have emerged to improve conventional engine overall efficiency and fuel economy to meet the requirements of clean and efficient diesel engines. As oxygen (O_2) has an important effect on the combustion process, some researchers have studied its impact on diesel combustion by increasing the oxygen concentration in the intake charge [1-2]. It is well known that using oxygen-enriched air leads to faster burn rates and accelerates the rate of heat release which can result in increasing combustion efficiency and power output. Studies on oxygen-enriched air found that a slight increase of oxygen makes a remarkable decrease in smoke emissions as well as a decrease in carbon monoxide (CO), unburned hydrocarbon (UHC), and PM emissions in diesel engine applications. However, a significant increase in NOx emissions has also been reported in these studies. For this reason, various techniques such as the utilization of EGR/diluent additions, injecting high-pressure water into the combustion chamber, and optimized injection strategies have been proposed to control NOx emissions [3-5]. Hountalas *et al.* [4] analyzed the effects of oxygen-enriched air on a heavy-duty diesel engine. They initially considered the engine operating conditions in a range from 21 to 25 vol.% of intake oxygen fraction. The results showed a remarkable reduction of particulate matter and slight improvement of Brake Specific Fuel Consumption (BSFC) while a significant increase of NOx emissions has been observed which caused the motivation to analyze the combination of EGR with oxygen-enriched combustion. For this purpose, they applied high pressure cooled EGR from 0 to 30 vol.%. Their results showed a considerable reduction of PM and NOx emissions accompanied by a limited penalty in BSFC. In 2018, Zhao *et al.* [5] studied the influences of

using oxygen-enriched air on combustion characteristics and emissions in a diesel engine. They have reported that by increasing intake oxygen concentration, PM emissions have inhibited while NOx emissions increase significantly. Increasing intake air humidification can reduce NOx emissions whereas it has some negative effects on PM emissions and indicated power.

In recent years, oxy-fuel combustion and nitrogen-free combustion coupled with Carbon Capture and Storage (CCS) techniques have been proposed as an efficient method to achieve carbon-free emissions and improve combustion efficiency. While most of the previous and ongoing oxy-fuel combustion technologies have focused on large-scale gas turbines or coal-fired power plants, which normally have up to 30% penalty on system energy efficiency [6-9], Internal Combustion (IC) engines, as the main power producers in the transportation sector, with the utilization of oxy-fuel combustion and CCS technology is of great significance. In oxy-fuel combustion, pure oxygen is used for combustion instead of air or enriched-oxygen air. Because there is no nitrogen in the intake charge, NOx emissions will be totally eliminated. Therefore, the resultants of the combustion reaction are only carbon dioxide and water vapor. The oxy-fuel application in IC engines was initially proposed by Osman in 2009 [9]. In that work, a water injection system was also applied to control the in-cylinder temperature and to enhance the heat absorption during the combustion process. In 2017, Kang *et al.* [10] conducted an experimental investigation to analyze the effects of oxy-fuel combustion and EGR on an HCCI engine. In their research, EGR was simulated by mixing CO_2 and H_2O in a surge tank prior to entering the cylinder. A water injection system was also utilized to examine the potential of abnormal mitigation. Their results show that injecting high pressure and high temperature water with proper injection timing can control the abnormal combustion. In addition, it helps to increase the engine's thermal efficiency.

Using oxy-fuel combustion enables the increasingly expensive and complicated NOx after-treatment systems to be completely eliminated. It also offers good fuel economy and very low levels of particulate emissions. However, using pure oxygen instead of air will accelerate the combustion process. As a result,

the ignition delay will be shortened. At the same time, premixed combustion is minimized while diffusion combustion is maximized. With the heat release rate dramatically increased, it takes a much shorter time to complete the entire heat release process. With such a high heat release rate, the flame temperature is expected to increase by around 500-800K. This necessitates a set of countermeasures to avoid overheating problems [9-12]. Most of these technologies can be classified in the category of advanced Low Temperature Combustion (LTC). One promising method to achieve LTC concept is Homogeneous Charge Compression Ignition (HCCI). Since HCCI has been introduced by Onishi et al. [13] in 1978 under the name of ATAC (Active Thermo-Atmosphere Combustion), it has been widely studied by many researchers over the last four decades. The relatively low temperatures achievable with HCCI combustion offer very low engine-out oxides of nitrogen (NOx). In addition, a homogeneous mixture in HCCI results in minimizing Particulate Matter (PM) emissions. However, HCCI suffers from several technical difficulties that require to be solved [14-15]. The main problem associated with HCCI lies in controlling the combustion phasing and the rate of heat release. In addition, low combustion temperature can also cause incomplete conversion of fuel to CO_2, thereby reducing efficiency and increasing CO and HC emissions. To solve these shortcomings, a large number of combustion control strategies have been proposed and examined both experimentally and numerically that can be organized into four main categories including variable compression ratio [16-17], variable intake conditions [18-20], regulated Exhaust Gas Recirculation (EGR) [21-24] and adjustable fuel blends [25-28].

As mentioned earlier, the application of oxy-fuel combustion with CCS technology has been mainly used on gas turbines and power plants and only a few studies have attempted to apply this strategy on IC engines. The current CFD study has been performed as a part of a European project named RIVER to explore the effects of oxy-fuel combustion on combustion characteristics and engine operating conditions in a diesel engine under the Homogenous Charge Compression Ignition (HCCI) mode. Compared to the internal combustion Rankine cycle (ICRC) engine which was applied by Fu [12] and oxy-fuel combustion systems

proposed by Osman [9] and promoted by Kang [10-11], the significant advantage of the current study is that EGR technology accompanied with HCCI combustion is used to control the oxy-fuel combustion process instead of water, which can prevent the shortage of the water injection process, such as lubrication and corrosion problems.

2. RIVER Project Proposed Technology

The main objective of the RIVER project is to eliminate NOx emissions and to capture and store carbon emissions from the IC engines used for inland boats. RIVER aims to address these issues by applying CCS technology and oxy-fuel combustion. Figure 1 shows a schematic view of the RIVER proposed technology.

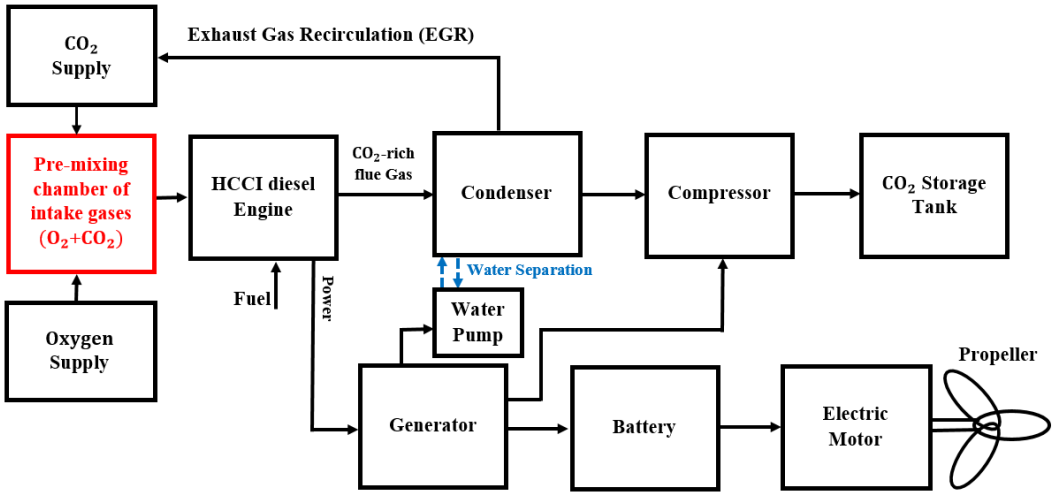

Figure 1 - Schematic view of the RIVER technology

As illustrated in Figure 1, the powertrain system used in the boat is a diesel generator. The engine works under HCCI combustion mode. The oxyfuel combustion configuration includes the oxygen supply system, the EGR system, and the CCS system. In the RIVER project, the oxygen is supplied from a commercial high-pressure oxygen cylinder. The exhaust gas, which mainly contains CO_2-rich flue gas is condensed, followed by the separation of water in a condenser. Subsequently, a portion of remained CO_2 is recirculated back through an EGR system and it is mixed with O_2 in a pre-mixing chamber before being fed into the engine. Meanwhile, the rest CO_2 is then compressed and stored in a storage tank. By performing this technology, it is expected that all carbon dioxide is stored while NOx emissions is completely eliminated.

This technology can be also applied to other sectors like heavy-duty vehicles, with appropriate space for a storage tank and oxy-fuel combustion setup. In order to optimize the oxy-fuel HCCI combustion project, it is required to adopt the appropriate ratio for the oxygen concentration and EGR rate. In the current study, the effects of different percentages of O_2 and CO_2 have been analyzed in detail to explore the effects of these parameters on combustion characteristics and engine operating conditions of a diesel engine under HCCI combustion mode.

3. Engine Specifications

A High-Speed Direct Injection (HSDI) common-rail diesel engine is used in this study. The specifications of the engine and the injection system are given in Table 1 and Table 2, respectively. The experimental test was done on a single cylinder of this engine at 1500 rev/min and 6.8 bar IMEP (Indicated Mean Effective Pressure) [29].

Table 1 - Engine Specification [29]

Model	Ford Puma DuraTorq
Type	4 Cylinder, 4 stroke diesel engine
Combustion chamber	Bowl in piston
Valves per cylinder	4
Bore [mm] × stroke [mm]	86 × 86
Squish Height [mm]	0.86
Comperation ratio	18.2:1
Displacement [cm^3]	1998
Connecting rod length [mm]	155
Peak cylinder pressure [MPa]	18
Swirl ratio	1.7
IVC [ABDC]	37°
EVO [ATDC]	-49°

Table 2 - Common rail injector specifications [29]

Injection system	Common rail DI [up to 180 MPa]
Injector	Solenoid with 6 holes
Injector hole diameter [mm]	0.159
Injection angle	154°
Fuel type	Diesel (D1)
Fuel temperature [K]	310

4. CFD Model Description

As diesel is used as fuel for this numerical research, a reduced chemical mechanism with 349 reactions and 76 species is employed to study the oxy-fuel combustion under HCCI combustion mode [30]. This mechanism has been shown to yield acceptable results in numerous studies (e.g., Mobasheri *et al.* [31]). A CFD model was built in the AVL Fire platform which allows 3D CFD simulation of the engine using different sub-models, coupled with detailed chemistry calculation [32].

To simulate the injection system with a high degree of atomization, KH-RT break-up model used which described in ref. [33] for the primary and secondary atomization modeling of the resulting droplets. In this model Kelvin-Helmholtz (KH) surface waves and Rayleigh-Taylor (RT) disturbances should be in continuous competition of breaking up the droplets. The KH mechanism is favored by high relative velocities and high ambient density. The RT mechanism is driven by the rapid deceleration of the droplets causing the growth of surface waves at the droplet stagnation point. Also, the Nordin model [34] was used to take parcels collision into account. The Nordin model is an improvement of the O'Rourke approach, which overcomes the grid dependency. According to Nordin's model, a collision between two parcels occurs if their trajectories intersect and the intersection point is reached at the same time and within the spray integration step [32]. The Dukowicz model was applied for treating the heat-up and evaporation of the droplets, which is described in ref. [35]. This model assumes a uniform droplet temperature. In addition, the rate of droplet temperature change is determined by the heat balance, which states that the heat convection from the gas to the droplet either heats up the droplet or supplies heat for vaporization.

The k-zeta-f approach has been used to take account of turbulent effects. This model has been recently developed by Hanjalic, Popovac, and Hadziabdic [36]. The authors propose a version of an eddy viscosity model based on Durbin's elliptic relaxation concept. The aim of developing of the k-zeta-f model was to improve the numerical stability of the $\overline{v^2} - f$ model, which has become increasingly popular as empirical damping functions are removed due to the employment of an additional velocity scale $\overline{v^2}$ derived by using

an elliptic relaxation concept [14]. The original model introduces the wall boundary condition for the elliptic relaxation function f proportional to $1/y^4$ (y is a dimensionless wall distance) making computations more sensitive on very near wall cells. Hanjalic et al. [36] used an eddy viscosity model, which solves a transport equation for the velocity scale ratio $\overline{v^2}/k$ instead of $\overline{v^2}$ in order to achieve a more robust wall boundary condition for f-equation which introduce a new equation for f_{wall} and it is proportional to $1/y^2$. In comparison with $k-\varepsilon$ turbulence model, k-zeta-f model computing time is increased by up to 15% when compared with the computing time of $k-\varepsilon$ model calculations. K-zeta-f model is beneficial and accurate for the calculation of cells which are next to the wall. However, the cell next to the wall should reach a non-dimensional wall distance y^+ of 3 as a maximum. In order to keep grid comply with this requirement, the k-zeta-f model was used in conjunction with wall functions for turbulence modeling [32]. Popovac and Hanjalic [36] used the blending formula for the quantities specified at the cell next to the wall as:

$$\Phi_P = \Phi_V e^{-\Gamma} + \Phi_t e^{-1/\Gamma} \quad (1)$$

Where v is the viscous and t the fully turbulent value of the variables: wall shear stress, production, and dissipation of the turbulence kinetic energy. In turbulence modeling in CFD Fire code, the k-zeta-f model is used in conjunction with the hybrid wall treatment and standard wall function for wall treatment and heat transfer wall models. It must be mentioned that multi-zone chemistry solving method was employed to decreasing the calculation time of combustion by considering computational meshes with similar properties into the same zone in calculations [37].

Figure 2 shows the computational grids at TDC.

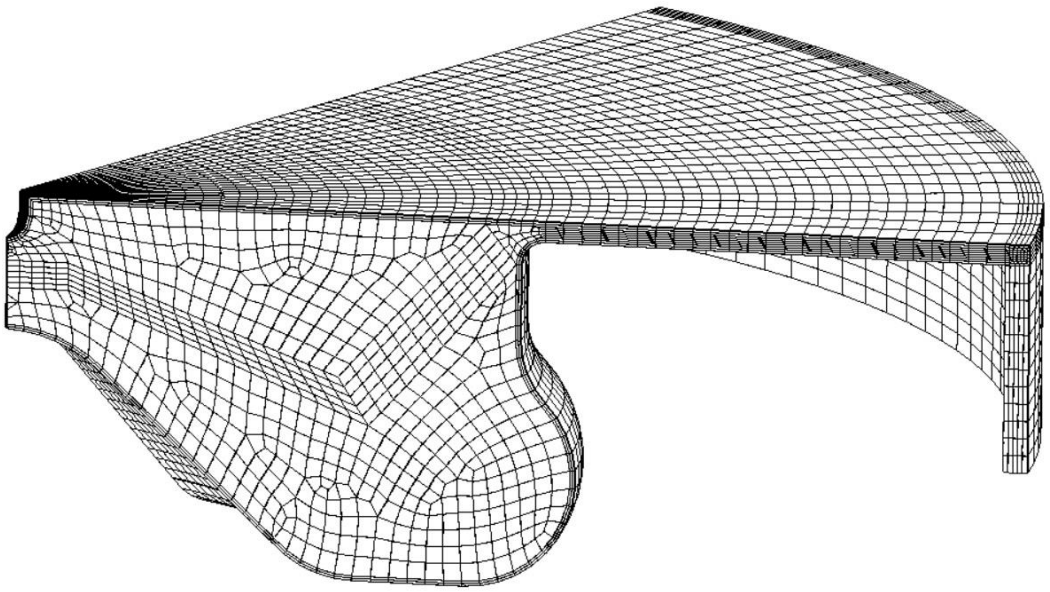

Figure 2 - Computational grids at TDC

As illustrated in Figure 2, to reduce calculation time, a 60° sector mesh (corresponding to the envelope zone of a single nozzle hole of the six-hole injector) is utilized for CFD simulation. In addition, the crevice above the top piston ring (between the piston and liner) is resolved and the region under the ring is represented as an additional volume attached to the top ring crevice. Furthermore, the volumes associated with the valve pockets and pressure transducer crevices are added to the volume attached to the top ring crevice in order to give the correct compression ratio.

The ground of the bowl meshed with three continuous layers for a proper calculation of the heat transfer through the piston wall. The exact number of cells in the mesh was 35240 and 90476 at Top Dead Center (TDC) and Bottom Dead Center (BDC), respectively.

5. Results and Discussion

5.1. Validation Study

Those experimental studies run at 1500 rev/min with three different EGR rates including 60.5%, 66.8%, and 69.6%, respectively, are used for the validation of the current CFD model. The operating conditions for these cases are given in Table 3 [29].

Table 3 - Engine operating conditions for preliminary study [29]

Parameter	EGR rate		
	60.5%	66.8%	69.6%
Engine speed [rev/min]	1500	1500	1500
IMEP [bar]	6.67	6.92	6.75
Fuel rate [mg/cycle]	5.1	5.1	5.1
Intake Pressure [bar]	2	2	2
Diesel injection pressure [MPa]	150	150	150
Number of injection [/cycle]	4	4	4
Diesel SOI [°CA]	@ 306, 314, 326, 338		
Injection Duration [μs/injection]	230	230	230
Indicated thermal efficiency [%]	38.1	39.1	38.6
Combustion efficiency [%]	98.6	97.8	97.1

The validation study was performed based on the conditions of Table 3. The measured and calculated mean in-cylinder pressure and rate of heat release (RoHR) at 60.5%, 66.8%, and 69.6% EGR rates are illustrated in Figure 3. In this study, 360° CA represents the piston position at the TDC.

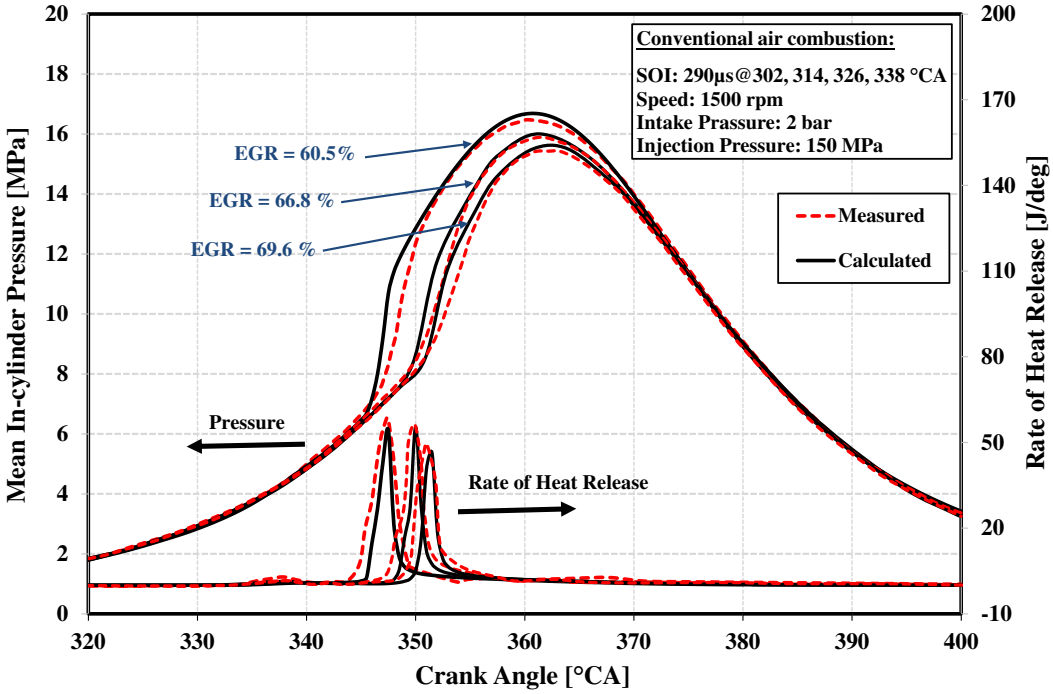

Figure 3 - Comparison of measured and calculated in-cylinder pressure and RoHR

As can be seen in Figure 3, the ignition timing and in-cylinder peak pressure are well predicted by the applied mechanism and the simulations are seen to be able to capture the combustion characteristics reasonably well. Although there are still some discrepancies in magnitudes, as can be seen in Figure 3.

These discrepancies could be mainly due to the uncertainty of some experimental data, especially the parameters that cannot directly measured such as wall cylinder temperature and piston surface temperature or can be related to experimental uncertainties in input parameters to the computations such as the precise start of injection timing and injection duration.

Table 4 shows comparisons of the measured and calculated engine-out NOx, PM, and CO emissions for three different EGR rates. The simulation capture NOx and PM magnitudes very well. However, CO is slightly over predicted. Since a majority of CO resides in the near wall and crevice zones, it is likely that CO levels may be sensitive to wall temperature.

Table 4 - Measured and calculated engine-out emissions for different EGR rates

Emission	EGR rate					
	60.5%		66.8%		69.6%	
	Measured	Calculated	Measured	Calculated	Measured	Calculated
NOx [ppm]	22.0	24.0	13.0	15.0	13.0	14.0
PM [g/kWh]	0.000200	0.000270	0.000700	0.000740	0.000800	0.000850
CO [ppm]	2440	2510	4290	4300	6350	6380

5.2. Oxy-fuel Combustion under HCCI Mode

The results of the previous section showed that the CFD model is able to adequately capture the combustion characteristics of Oxy-fuel HCCI combustion. In this section, the 3-D CFD model with the chemical mechanism has been used to investigate the effects of oxy-fuel combustion under HCCI combustion mode. During this phase of the study, the engine speed was maintained at 1500 rev/min while the engine loads were varied by changing the fuel injection rates. Other operating parameters of the engine such as injection timing, initial conditions, intake pressure, and intake temperature were held constant. Table 5 shows percentages of O_2 and CO_2 vol.% for different diluent strategies, the mass of the injected fuel, the relative O_2-fuel ratio ($Lambda_{O_2}$), and lambda for each strategy. Investigations have conducted using four different diluent strategies based on the volume fraction of O_2 and a diluent gas (CO_2). It should be noted, in this study, since a mixture of O_2 and CO_2 have been used instead of air, the “lambda” determines the ratio

between the actual amount of O_2 + CO_2 vs. the stoichiometric mixture. In addition, in Table 5, relative O_2-fuel ratio ($Lambda_{O_2}$) is defined using Equation. 2.

$$Lambda_{O_2} = \frac{\text{Actual } O_2\text{−fuel ratio}}{O_2\text{−fuel ratio for stoichiemetric combustion}} \quad (2)$$

Table 5 - Outlook of different studied diluent strategies

Case study (vol.%)	Fuel injection per cycle (mg)	$Lambda_{O_2}$ (Relative O_2-fuel ratio)	Lambda
23% O_2 + 77% CO_2	5.2	2.38	2.85
	4.4	2.82	3.37
	4	3.10	3.71
	3.6	3.44	4.12
	3.2	3.87	4.63
	2.8	4.43	5.30
21% O_2 + 79% CO_2	5.2	2.18	2.87
	4.4	2.57	3.39
	4	2.83	3.73
	3.6	3.14	4.14
	3.2	3.54	4.66
	2.8	4.04	5.33
19% O_2 + 81% CO_2	5.2	1.97	2.88
	4.4	2.33	3.41
	4	2.56	3.75
	3.6	2.84	4.17
	3.2	3.20	4.69
	2.8	3.66	5.36
17% O_2 + 83% CO_2	5.2	1.77	2.90
	4.4	2.09	3.43
	4	2.30	3.77
	3.6	2.55	4.19
	3.2	2.87	4.71
	2.8	3.28	5.39

In this research, the CO_2 volume fraction intake was varied between 77% and 83%. In addition, the mass fraction of CO_2 and O_2 in the intake charge has achieved using Equations 3 and 4, respectively.

$$CO_2(\text{mass fraction}) = \frac{\rho_{CO_2} \cdot V_{CO_2}}{\rho_{CO_2} \cdot V_{CO_2} + \rho_{O_2}(1 - V_{CO_2})} \quad (3)$$

$$O_2(\text{mass fraction}) = 1 - CO_2(\text{mass fraction}) \quad (4)$$

Where V_{CO_2} is the volume percentage of CO_2 and ρ_{CO_2} and ρ_{O_2} are the density of CO_2 and O_2, respectively. The first series of investigations was performed at a constant fuel injection rating at which 4.4 mg of fuel is injected per cycle.

Effects of different diluent strategies on mean in-cylinder pressure, in-cylinder temperature, and accumulated heat release rate are shown in Figures 4, 5, and 6, respectively.

As illustrated in Figures 4 and 5, increasing O_2 concentration lead to increase the peak of in-cylinder pressure and in-cylinder temperature. The maximum in-cylinder temperature is achieved from the highest inlet O_2 concentration. This suggests that by increasing O_2 concentration from 17% to 23%, the ignition delay is shortened and fuel is burned more rapidly which results in a shorter combustion period.

As can be seen in Figure 5, when the diluent ratios increase from 77% to 83%, the in-cylinder peak temperature drops from 1414 K to 1312 K.

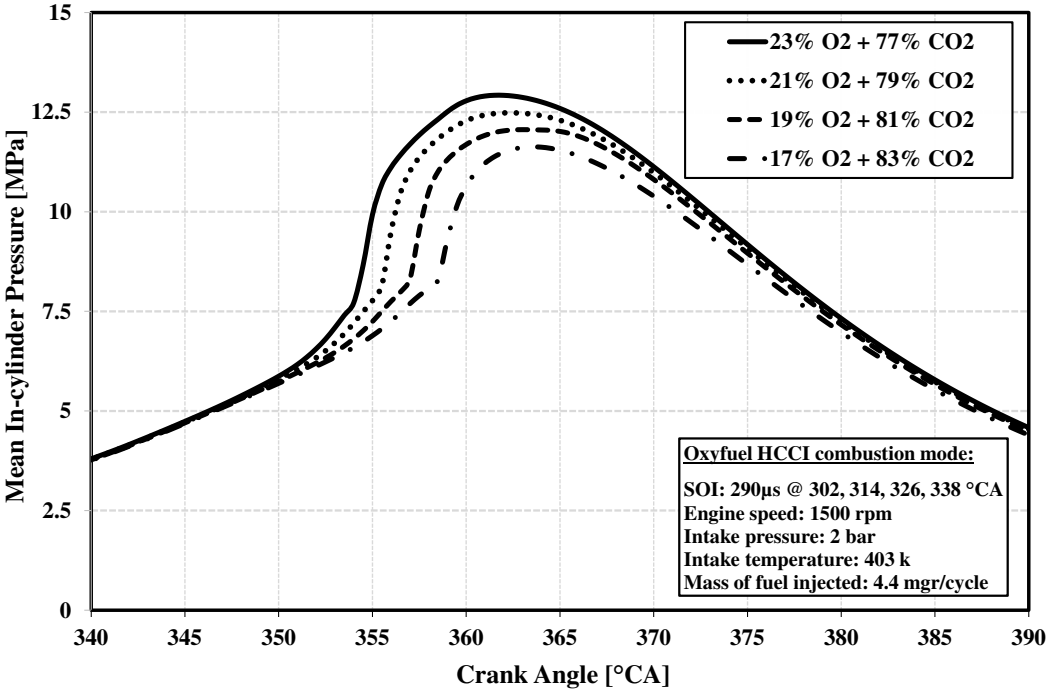

Figure 4 – Mean in-cylinder pressure for different diluent strategies under oxy-fuel combustion mode

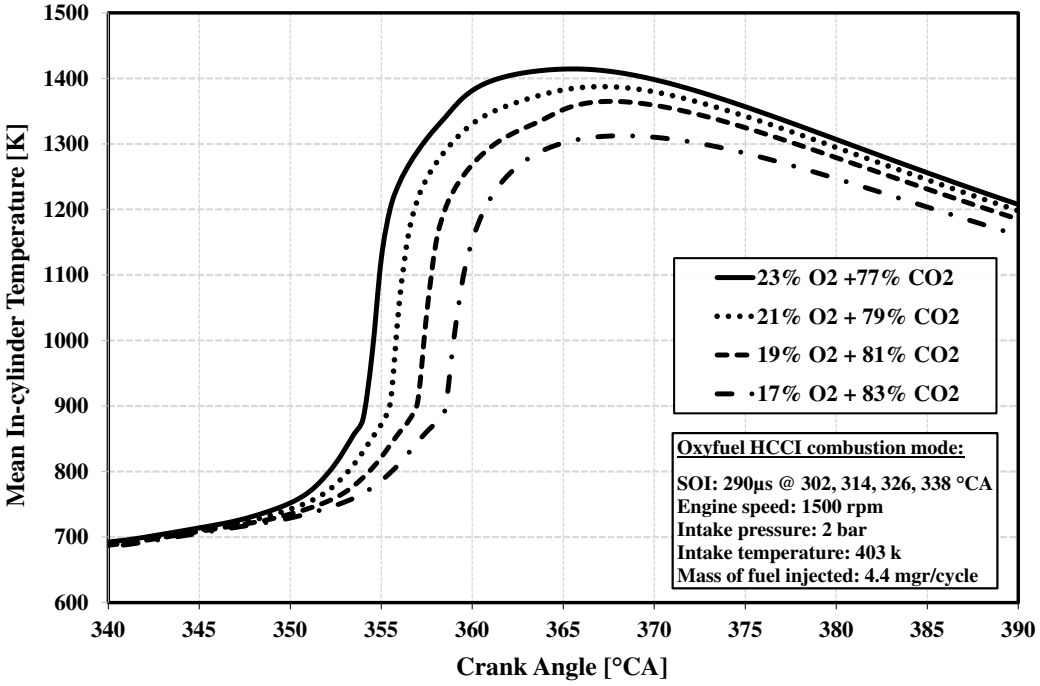

Figure 5 – Mean in-cylinder temperature for different diluent strategies under oxy-fuel combustion mode

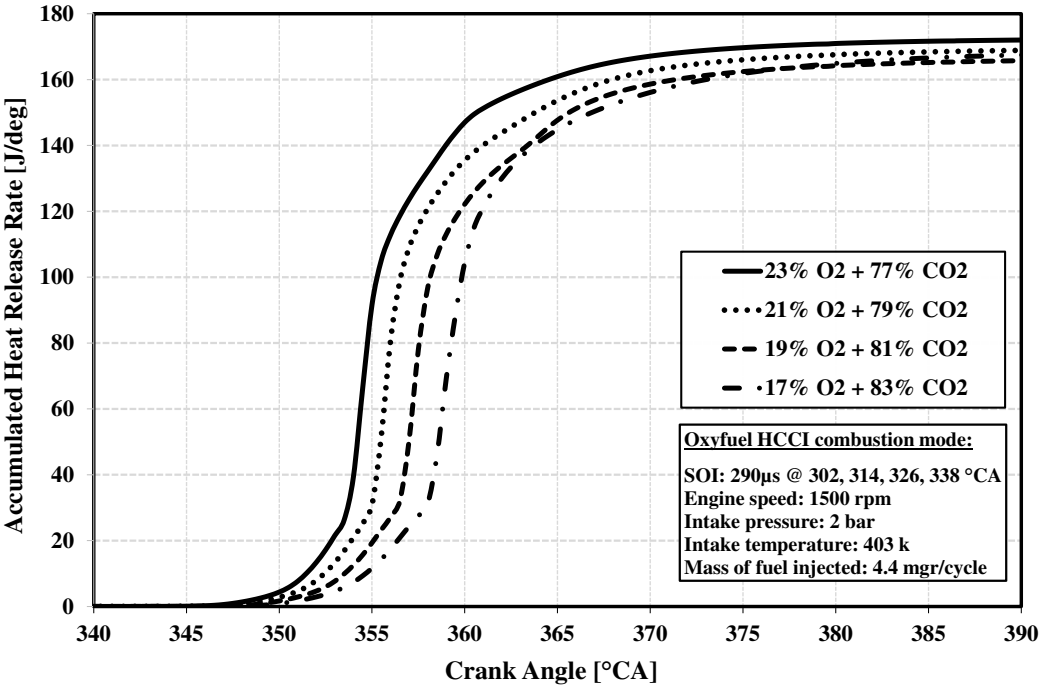

Figure 6 – Accumulated heat release rate for different diluent strategies under oxy-fuel combustion mode

According to Figure 6, the highest value of accumulated heat release rate is achieved when the 23% of inlet oxygen is applied. This effect can be also attributed to the increase of burning rate of the injected fuel mass with increasing intake oxygen fraction due to higher oxygen availability during the premixed and diffusion

combustion. It should be pointed out that the amount of PM emissions for all studied cases was at ultra-low level (<0.0004 gr/kg.fuel) while NOx emissions was completely eliminated using oxy-fuel HCCI combustion mode.

In order to determine the effects of applied strategies on engine performance and combustion characteristics, in the second series of investigations, five different amounts of diesel injected mass have been considered to evaluate the operating range of oxy-fuel HCCI combustion.

Figure 7 shows the effects of different studied cases on IMEP. The horizontal axis represents the overall air-fuel equivalence ratio (lambda) of the cylinder charge.

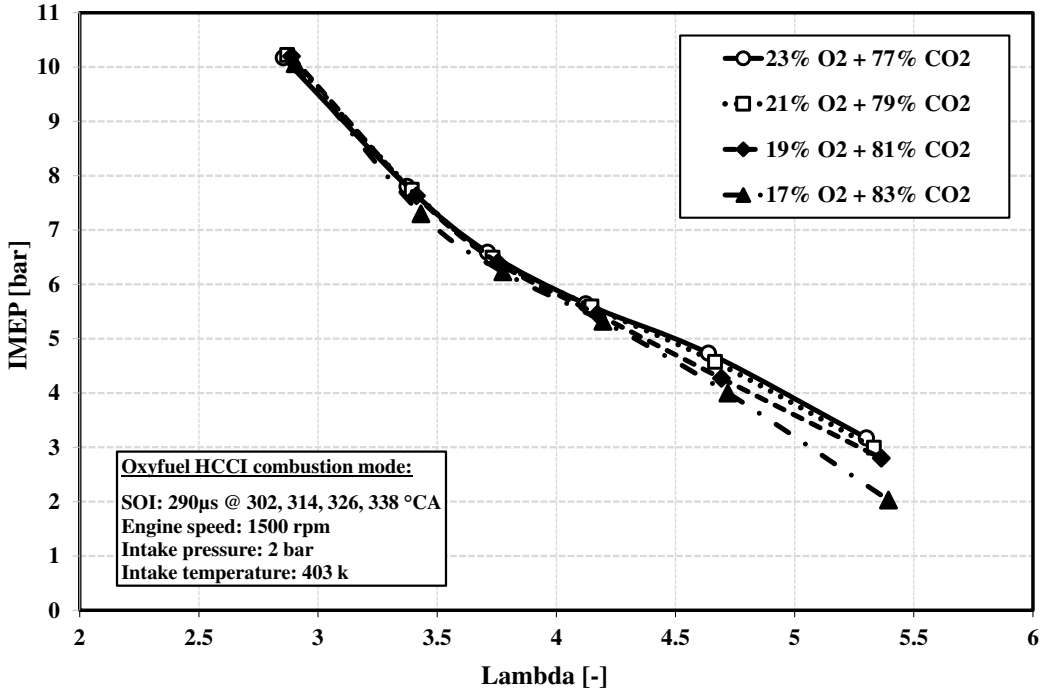

Figure 7 – Effects of different diluent ratios on IMEP

As illustrated in Figure 7, the increase of diluent ratio from 77 to 83 vol.% under constant fueling rate does not bring any remarkable change to the IMEP at high engine loads (small lambda). It indicates that, at high engine loads, using a high diluent ratio did not affect IMEP too severely. However, by decreasing the fuel rate (higher lambda) the difference between different diluent strategies becomes more obvious as the minimum amount of IMEP is achieved when 83 vol.% of CO_2 is used in the intake charge.

Figure 8 shows the effects of different studied cases on Indicated Thermal Efficiency (ITE). According to Figure 8, increasing the CO_2 concentration results in a decrease in ITE. It can be seen that the thermal efficiency is very sensitive to the percentage of diluent ratio at low engine loads. The indicated thermal efficiency was reduced from 32.7% to 20.9% as the CO_2 concentration was increased from 77% to 83%. It can be concluded that CO_2, as a triatomic molecule, has a larger specific capacity compared to a diatomic molecule, i.e. O_2. Therefore, applying the higher percentage of CO_2 will greatly increase the overall specific heat capacity of the intake charge which leads to decrease of temperature and consequently, the cylinder pressure during combustion process results in lower indicated power and ITE.

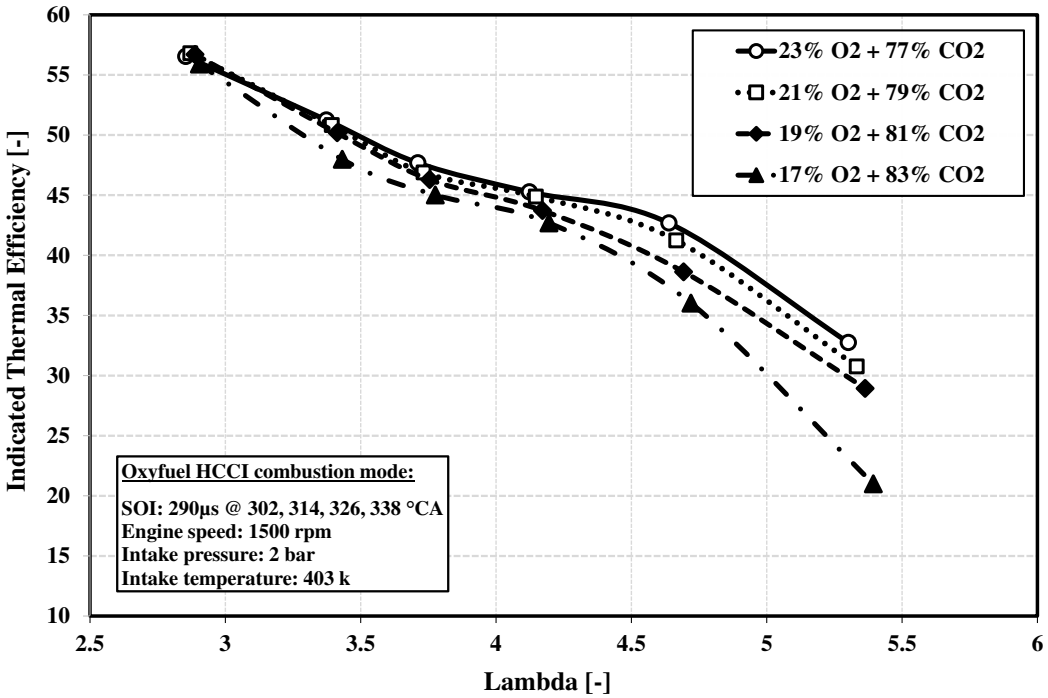

Figure 8 – Effects of different diluent ratios on indicated thermal efficiency

Table 6 shows the amount of CO and PM emissions and O_2 in the exhaust gas.

Table 6 – Effects of different diluent strategies on PM and CO emissions and O_2 in the exhaust gas

Applied diluent strategy	Fuel mass per cycle [mgr]	$Lambda_{O2}$ [-]	PM [gr/kg.fuel]	CO [gr/kg.fuel]	Exhaust O_2 [kg/kg.fuel]
23% O_2 + 77% CO_2	5.2	2.38	1.92E-04	59.25	4.14
21% O_2 + 79% CO_2	5.2	2.18	1.17E-04	72.57	3.50
19% O_2 + 81% CO_2	5.2	1.97	3.66E-05	86.14	2.86
17% O_2 + 83% CO_2	5.2	1.77	3.88E-05	161.8	2.28

The results obtained in Table 6, indicate that the oxy-fuel HCCI combustion has brought the CO and PM emissions to a very ultra-low level while the NOx emission has been completely eliminated using the oxy-fuel combustion.

In order to further analysis of the effects of oxy-fuel HCCI combustion on combustion characteristics, effects of diluent strategies on the start of combustion (CA10), the combustion phasing (CA50), the combustion duration and CA90 have been considered in the following section. CA10 or the start of combustion (SOC) is defined as the crank angle position at which 10% of total fuel energy has been released, while CA90 is defined as the crank angle position at which 90% of total fuel energy has been released. In addition, combustion duration or burn duration is defined as the period between CA10 and CA90 (CA90 – CA10).

Figure 9 illustrates the variations of CA10 in oxy-fuel HCCI combustion mode for different diluent strategies.

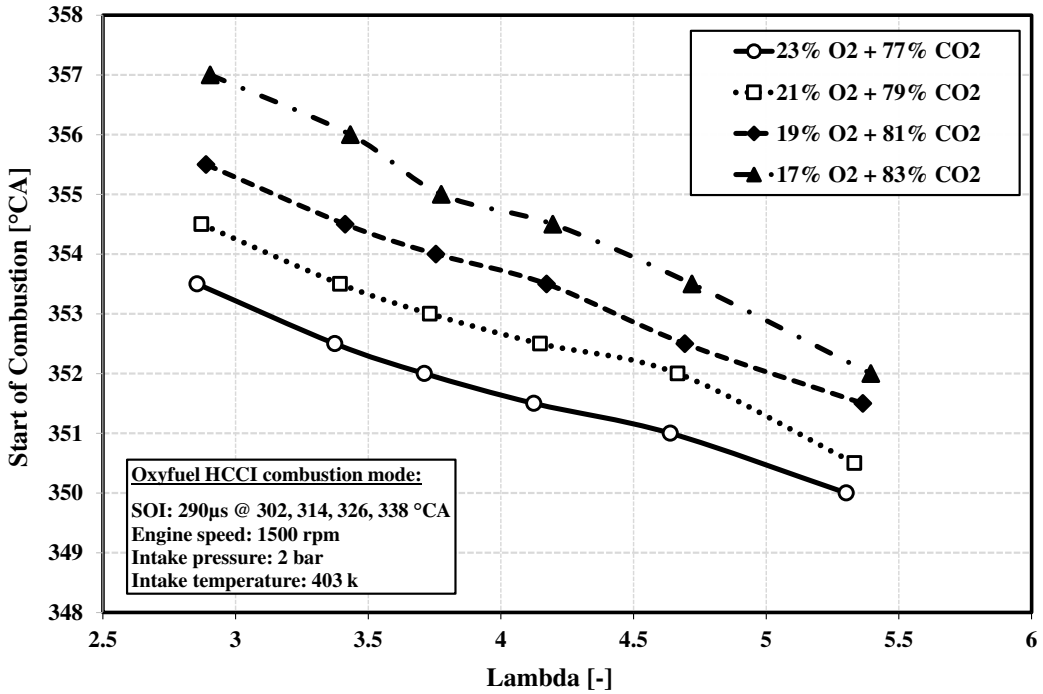

Figure 9 – Influence of oxy-fuel HCCI combustion on CA10 for different diluent strategies

As can be seen in Figure 9, by increasing the O_2 concentration in the range of 17 to 23 vol.%, CA10 advances over the whole range of loads. It can demonstrate that increasing O_2 concentration results in increasing the speed of reaction kinetics which leads to an earlier auto-ignition process and higher in-cylinder temperature. In addition, it was found that using further CO_2 concentration in a diluent strategy leads to late auto-ignition. As a result, the main combustion process will take place near the end of the compression stroke and therefore, the output power is more reduced.

Figure 10 shows the effect of oxy-fuel HCCI combustion on CA50. As can be seen in Figure 10, at high fulling rates, increasing CO_2 ratio in intake charge from 77 to 83 vol.% retards the CA50 by around 5°CA. In addition, for every 2% increase in the O_2 concentration, the combustion phasing was advanced by around 2 CAs. A similar trend in terms of the variation at the start of combustion was observed in Figure 9. As CO_2 concentration increases, the mean in-cylinder temperature reduces further which leads to more delays in combustion phasing and later CA50s.

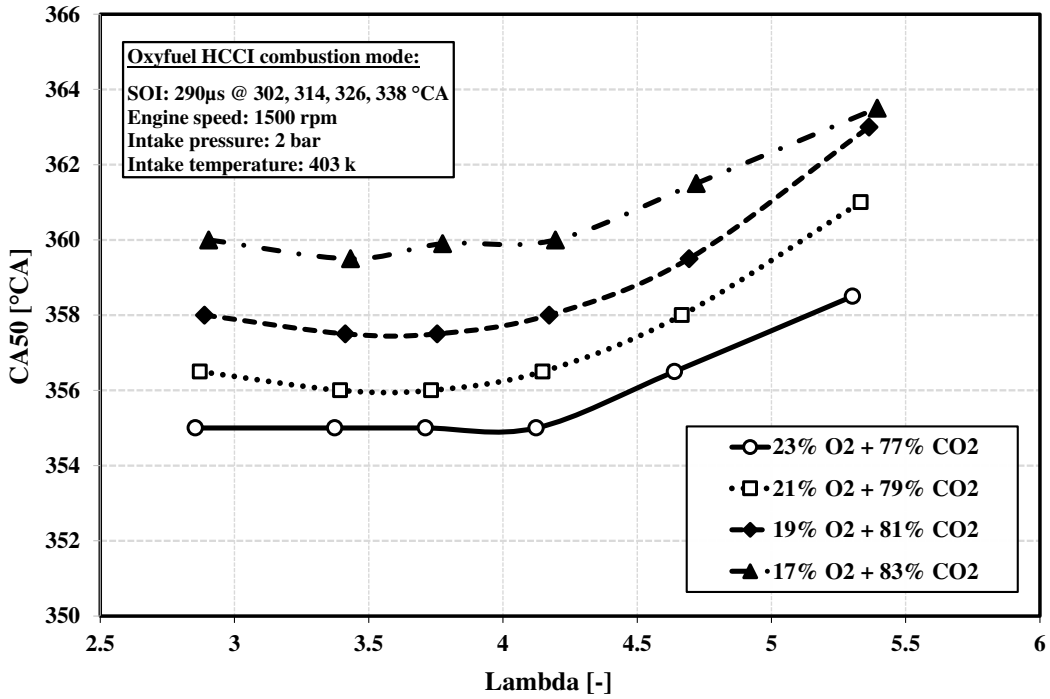

Figure 10 – Influence of oxy-fuel HCCI combustion on CA50 for different diluent strategies

Figure 11 illustrates the effects of diluent strategies on the combustion duration. As shown in Figure 11, the shortest combustion duration is 6° CA at lambda 2.85 as 23% of intake O_2 is applied. The maximum

duration of heat release is 25° CA at lambda 5.39 when 17% of intake O_2 is utilized. In addition, the results show that for the relatively fuel-rich mixtures (lambda range of 3.5-4.2), the effects of different diluent strategies on combustion duration was less noticeable.

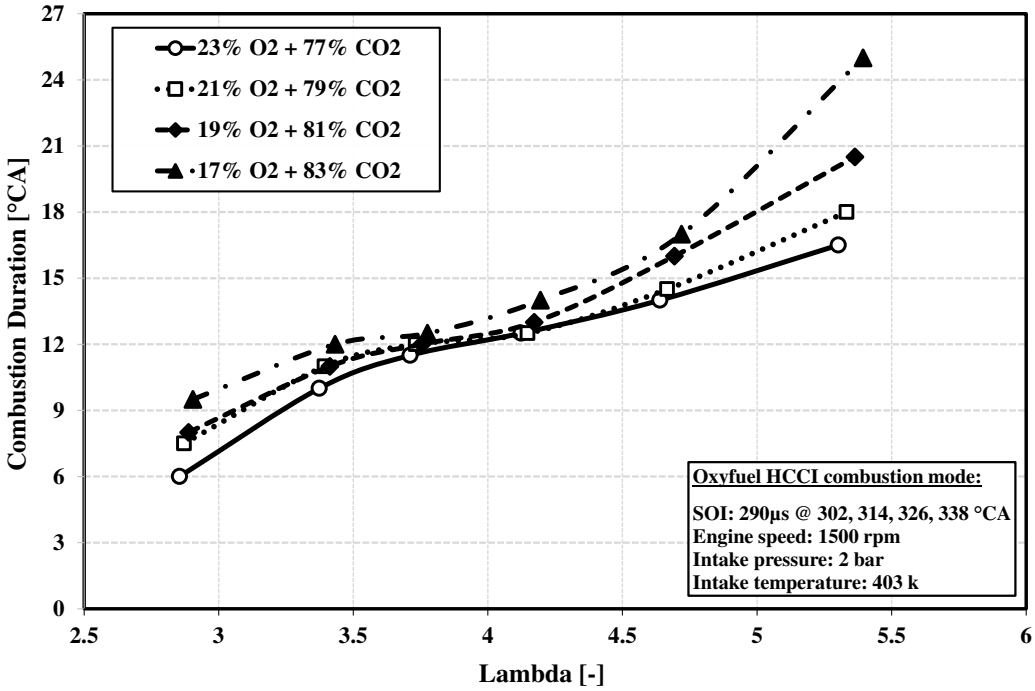

Figure 11 – Influence of oxy-fuel HCCI combustion on combustion duration for different diluent strategies

The effects of different diluent strategies on CA90 is shown in Figure 12. It can be seen that when the O_2 concentration has decreased from 23% to 17%, CA90 has retarded by around 4-6CAs, independent of the lambda value. Moreover, it is noted from Figure 11 and 12 that increasing O_2 concentration had less impact on the combustion duration than the CA90.

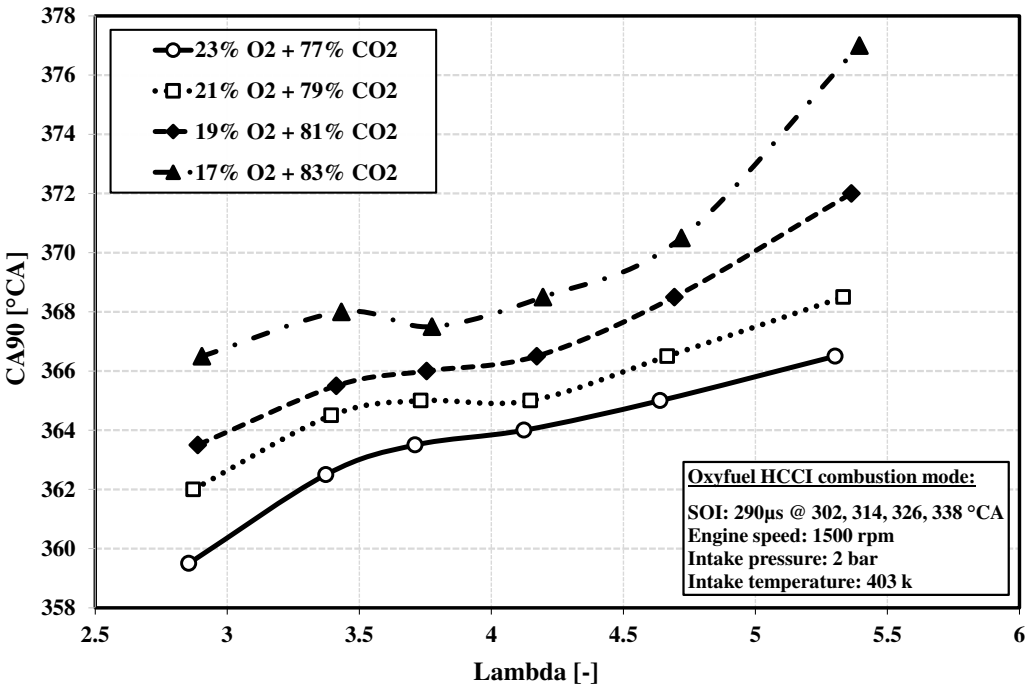

Figure 12 – Influence of oxy-fuel HCCI combustion on CA90 for different diluent strategies

Figure 13 shows the effect of three different diluent strategies on in-cylinder temperature distribution at 5, 10, and 20 °CA ATDC, respectively. It is observed that by increasing the inlet O_2 concentration, the maximum temperature inside the cylinder has increased due to more oxygen availability during the combustion process.

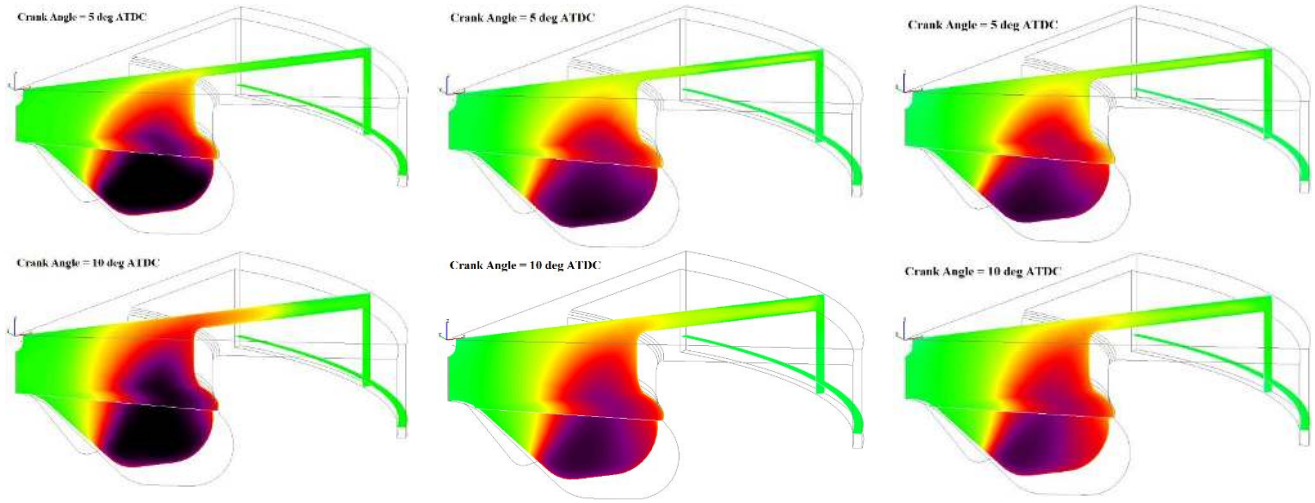

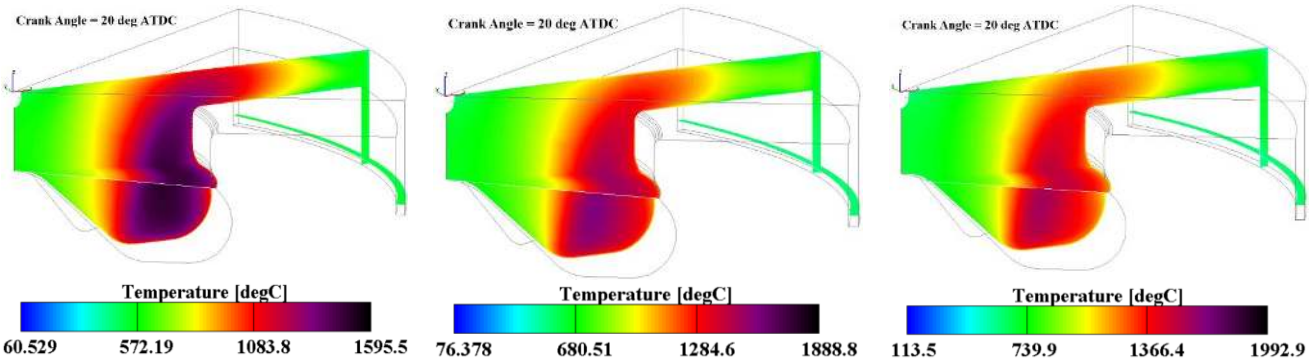

17% O_2 + 83% CO_2 19% O_2 + 81% CO_2 23% O_2 + 77% CO_2

Figure 13 – In-cylinder temperature distribution for three different diluent strategies

Figure 14 shows the comparison of OH radical distribution for three different diluent strategies. OH radical is one of the most important intermediate species during combustion that directly affects the soot formation and oxidation processes. As can be seen in Figure 14, the OH formation zone is mainly located in the bowl region. By increasing the diluent ratio, the OH formation has increased within the cylinder. Although the amount of OH for all cases is at a very low level.

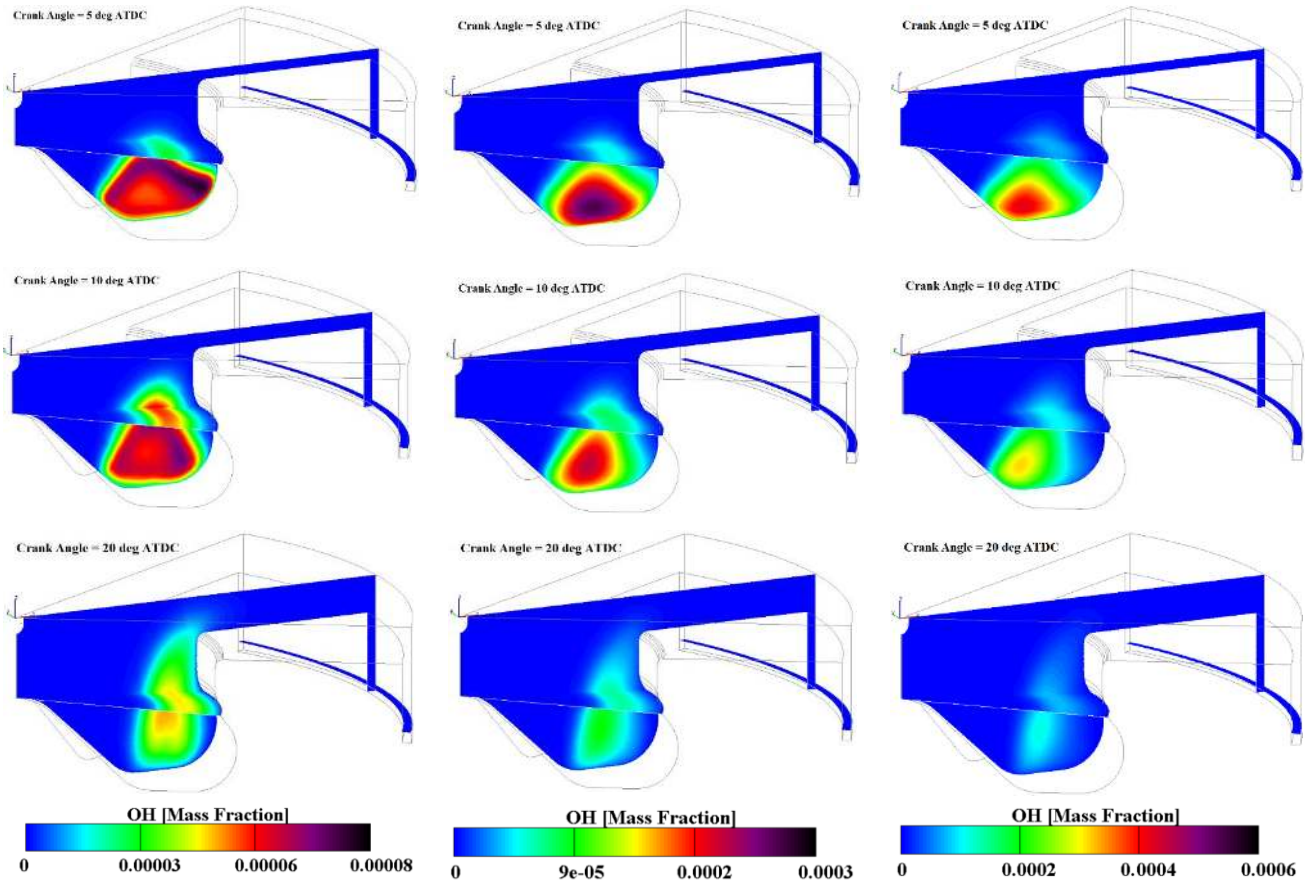

17% O_2 + 83% CO_2 19% O_2 + 81% CO_2 23% O_2 + 77% CO_2

Figure 14 – OH distribution for three different diluent strategies

Figure 15 illustrates the distribution of CO for three different diluent strategies.

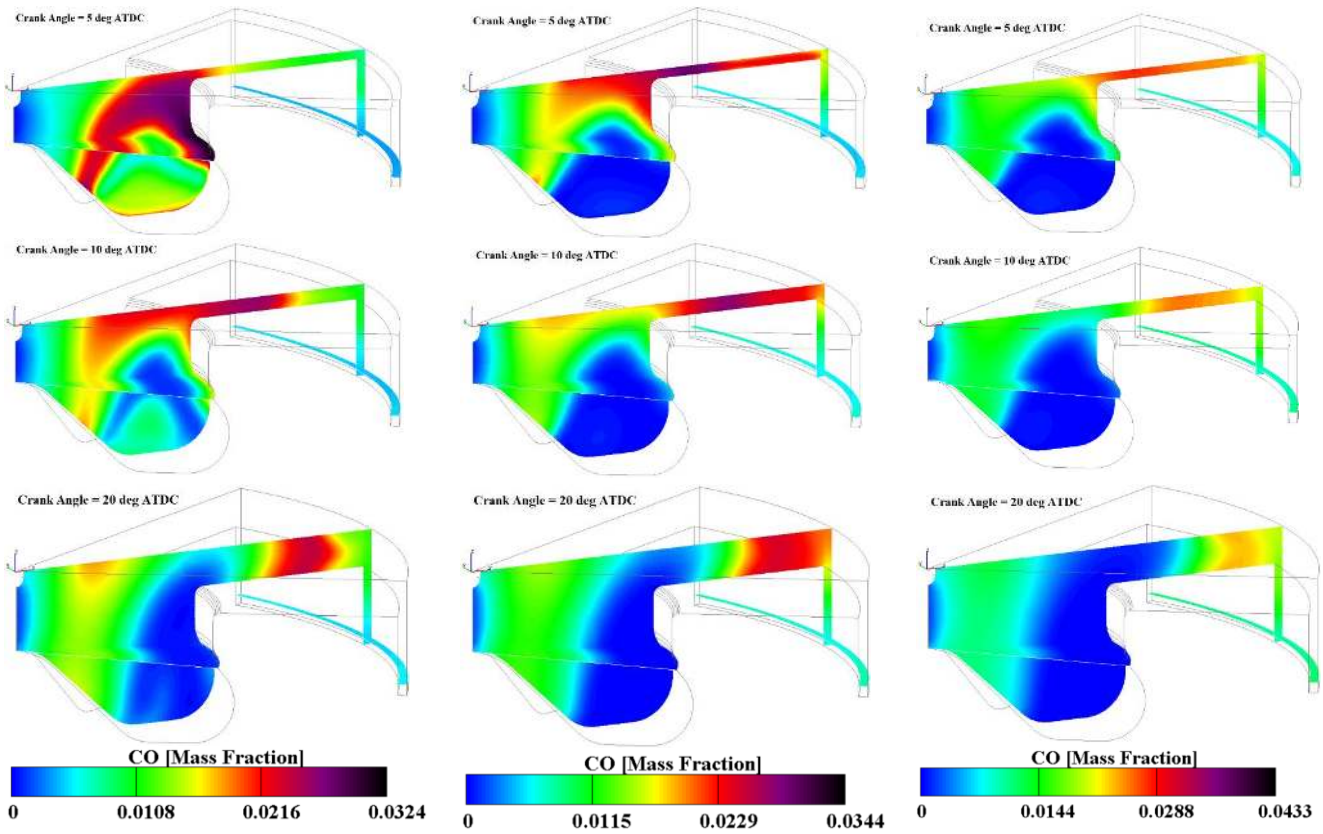

17% O_2 + 83% CO_2 19% O_2 + 81% CO_2 23% O_2 + 77% CO_2

Figure 15 – CO distribution for three different diluent strategies

It can be clearly seen from Figure 15 that by increasing O_2 concentration the amount of CO emissions has decreased. It may also due to the fact that by increasing O_2 concentration, due to shorter ignition delay period, more evaporated fuel accumulated and burned in the diffusive mode which leads to higher maximum in-cylinder temperature and in-cylinder pressure which could lead to more complete combustion and less CO formation.

6. Summary and conclusion

The effects of oxy-fuel combustion have been computationally investigated under HCCI combustion mode. Simulation was carried out on an HSDI diesel engine. A reduced chemical mechanism with 349 reactions and 76 species has employed for oxy-fuel HCCI combustion modeling. Variation in the diluent

ratio has achieved by adding different percentages of CO_2 for a range from 77 to 83 vol. %. The results discussed in this paper have suggested that the oxy-fuel HCCI combustion has the potentials to bring PM and CO emissions to a very ultra-low level while the NOx emissions can be completely eliminated.

The major results of this study can be summarized as follows:

1. By increasing O_2 concentration from 17% to 23%, under a constant fueling rate, the ignition period is shortened and fuel is burned more rapidly which results in a higher in-cylinder temperature and in-cylinder pressure.
2. The increase of diluent ratio from 77 to 83 vol.% under constant fueling rate does not bring any remarkable change to IMEP at high engine loads. However, by decreasing the fuel rate, the difference between different diluent strategies become more obvious as the minimum amount of IMEP is achieved when 83 vol.% of CO_2 is used in the intake charge.
3. The indicated thermal efficiency has reduced from 32.7% to 20.9% as the CO_2 concentration has increased from 77% to 83% at low engine loads. Applying a higher percentage of CO_2 will greatly increase the overall specific heat capacity of intake charge which leads to a decrease in temperature and consequently, the cylinder pressure during the combustion process results in lower indicated thermal efficiency.

References

[1] Manenti, F., Milani, M., Montorsi, L., Paltrinieri, F. *et al*., "Performance and Exhaust Emissions Analysis of a Diesel Engine Using Oxygen-Enriched Air," SAE Technical Paper 2018-01-1785, 2018, https://doi.org/10.4271/2018-01-1785.

[2] Zhang, W., Zhaohui, C., Weidong, L., Gequn, S. et al., "Influence of EGR and Oxygen-Enriched Air on Diesel Engine NO-Smoke Emission and Combustion Characteristic," Applied Energy 107:304-314, 2013, doi:10.1016/j.apenergy.2013.02.024.

[3] Wang, Y., Feng, L., Geng, C., Chen, B. et al., "Natural Flame Luminosity and Emission Spectra of Diesel Spray Flame under Oxygen-Enriched Condition in an Optical Constant Volume Vessel," SAE Technical Paper 2018-01-1781, 2018, doi:10.4271/2018-01-1781.

[4] Hountalas, D., Raptotasios, S., Zannis, T., and Papagiannakis, R., "Phenomenological Modelling of Oxygen-Enriched Combustion and Pollutant Formation in Heavy-Duty Diesel Engines using Exhaust Gas Recirculation," SAE Int. J. Engines 5(4):1693-1708, 2012, https://doi.org/10.4271/2012-01-1725.

[5] Zhao, C., Wang, K., and Huang, S., "Numerical Investigation on Effects of Oxygen-Enriched Air and Intake Air Humidification on Combustion and Emission Characteristics of Marine Diesel Engine," SAE Technical Paper 2018-01-1788, 2018, https://doi.org/10.4271/2018-01-1788.
[6] Liu, C., Chen, G., Sipöcz, N., Assadi, M. *et al*., "Characteristics of Oxy-Fuel Combustion in Gas Turbines," Applied Energy 89(1):387-394, 2012, doi:10.1016/j.apenergy.2011.08.004.
[7] Kunze, C. and Hartmut, S., "Assessment of Oxy-Fuel, Pre and Post-Combustion-Based Carbon Capture for Future IGCC Plants," Applied Energy 94:109-116, 2012, doi:10.1016/j.apenergy.2012.01.013.
[8] Olumayegun, O., Wang, M., and Greg, K., "Closed-Cycle Gas Turbine for Power Generation: A State-of-the-Art Review," Fuel 180:694-717, 2016, doi:10.1016/j.fuel.2016.04.074.
[9] Osman, A., "Feasibility Study of a Novel Combustion Cycle Involving Oxygen and Water," SAE Technical Paper 2009-01-2808, 2009, https://doi.org/10.4271/2009-01-2808.
[10] Kang, Z., Chen, S., Wu, Z., Deng, J. *et al*., "Simulation Study of Water Injection Strategy in Improving Cycle Efficiency Based on a Novel Compression Ignition Oxy-Fuel Combustion Engine," SAE Technical Paper 2018-01-0894, 2018, doi:10.4271/2018-01-0894.
[11] Kang, Z., Wu, Z., Zhang, Z., Deng, J. *et al*., "Study of the Combustion Characteristics of a HCCI Engine Coupled with Oxy-Fuel Combustion Mode," SAE Int. J. Engines 10(3):908-916, 2017, https://doi.org/10.4271/2017-01-0649.
[12] Fu, L., Wu, Z., Yu, X., Deng, J., Hu, Z., & Li, L. (2015). Experimental Investigation of Combustion and Emission Characteristics for Internal Combustion Rankine Cycle Engine under Different Water Injection Laws. In Physics Procedia (Vol. 66, pp. 89–92). Elsevier B.V. https://doi.org/10.1016/j.egypro.2015.02.047.
[13] Onishi, S., Jo, S., Shoda, K., Jo, P. *et al.,* "Active Thermo-Atmosphere Combustion (ATAC) - A New Combustion Process for Internal Combustion Engines," SAE Technical Paper 790501, 1979, https://doi.org/10.4271/790501.
[14] Pacheco A.F., Martins M.E.S., Zhao H. New European Drive Cycle (NEDC) simulation of a passenger car with a HCCI engine: Emissions and fuel consumption results. Fuel 2013, 111, pp. 733-739.
[15] Shi L., Deng K., Cui Y., Qu S., Hu W. Study on knocking combustion in a diesel HCCI engine with fuel injection in negative valve overlap. *Fuel* 2013, 106 , pp. 478-483.
[16] Tojo, T., Yoshida, K., Iijima, A., Shoji, H. *et al*., "Analysis of the Effects of a Higher Compression Ratio on HCCI Combustion Characteristics using In-cylinder Visualization and Spectroscopic Measurement," SAE Technical Paper 2012-32-0078, 2012, https://doi.org/10.4271/2012-32-0078.
[17] M, M. and Krishnasamy, A., "Effects of Compression Ratio and Water Vapor Induction on the Achievable Load Limits of a Light Duty Diesel Engine Operated in HCCI Mode," SAE Technical Paper 2019-01-0962, 2019, https://doi.org/10.4271/2019-01-0962.
[18] Singh, A. and Agarwal, A., "Effect of Intake Charge Temperature and EGR on Biodiesel Fuelled HCCI Engine," SAE Technical Paper 2016-28-0257, 2016, https://doi.org/10.4271/2016-28-0257.
[19] Li, C., Yin, L., Shamun, S., Tuner, M. *et al*., "Transition from HCCI to PPC: the Sensitivity of Combustion Phasing to the Intake Temperature and the Injection Timing with and without EGR," SAE Technical Paper 2016-01-0767, 2016, https://doi.org/10.4271/2016-01-0767.
[20] Saigaonkar, H., Nazemi, M., and Shahbakhti, M., "Sequential Model for Residual Affected HCCI with Variable Valve Timing," SAE Technical Paper 2015-01-1748, 2015, https://doi.org/10.4271/2015-01-1748.
[21] Jung, D. and Iida, N., "An Investigation into Cycle-to-Cycle Variations of IMEP using External EGR and Rebreathed EGR in an HCCI Engine, Based on Experimental and Single-Zone Modeling," SAE Technical Paper 2015-01-1805, 2015, https://doi.org/10.4271/2015-01-1805.
[22] Takamura, Y., Shima, T., Suzuki, H., Agui, K. *et al*., "Influence of Supercharging and EGR on Multi-stage Heat Release in an HCCI Engine," SAE Technical Paper 2016-32-0009, 2016, https://doi.org/10.4271/2016-32-0009.

[23] Lin, Z., Takeda, K., Yoshida, Y., Iijima, A. *et al*., "Influence of EGR on Knocking in an HCCI Engine Using an Optically Accessible Engine," SAE Technical Paper 2016-32-0012, 2016, https://doi.org/10.4271/2016-32-0012.
[24] Mobasheri, R. and Khabbaz, S., "Modeling the Effects of High EGR Rates in Conjunction with Optimum Multiple Injection Techniques in a Heavy Duty DI Diesel Engine," SAE Technical Paper 2014-01-1124, 2014, doi:10.4271/2014-01- 1124.
[25] Lacey, J., Kameshwaran, K., Filipi, Z., Fuentes-Afflick, P., & Cannella, W. (2020). The effect of fuel composition and additive packages on deposit properties and homogeneous charge compression ignition combustion. International Journal of Engine Research, 21(9), 1631–1646. https://doi.org/10.1177/1468087419828624.
[26] Krishnasamy, A., Gupta, S. K., & Reitz, R. D. (2020). Prospective fuels for diesel low temperature combustion engine applications: A critical review. International Journal of Engine Research. https://doi.org/10.1177/1468087420960857.
[27] Truedsson, I., Rousselle, C., and Foucher, F., "Ozone Seeding Effect on the Ignition Event in HCCI Combustion of Gasoline-Ethanol Blends," SAE Technical Paper 2017-01-0727, 2017, https://doi.org/10.4271/2017-01-0727.
[28] Lacey, J., Kameshwaran, K., Filipi, Z., Fuentes-Afflick, P., & Cannella, W. (2020). The effect of fuel composition and additive packages on deposit properties and homogeneous charge compression ignition combustion. International Journal of Engine Research, 21(9), 1631–1646. https://doi.org/10.1177/1468087419828624.
[29] Reader, G. T., Asad, U. and Zheng, M. (2013), Energy efficiency trade-off with phasing of HCCI combustion. Int. J. Energy Res., 37: 200-210. https://doi.org/10.1002/er.1900.
[30] Wang, H.; Reitz, R. D.; Yao, M.; Yang, B.; Jiao, Q.; Qiu, L., Development of an n-heptane-n-butanol-PAH mechanism and its application for combustion and soot prediction. Combust. Flame 2013, 160, (3), 504-519.
[31] Mobasheri, R. and Seddiq, M., "Effects of Diesel Injection Parameters in a Heavy Duty Iso-Butanol/Diesel Reactivity Controlled Compression Ignition (RCCI) Engine," SAE Technical Paper 2018-01-0197, 2018, https://doi.org/10.4271/2018-01-0197.
[32] ICE Physics & Chemistry, AVL FIRE user Manual v.2018.1, 2018.
[33] Su, T.F., Patterson, M.A., Reitz, R.D. and Farrell, P.V. “Experimental and Numerical Studies of High Pressure Multiple Injection Sprays”, SAE 960861, 1996.
[34] Nordin, N. “Complex Chemistry Modeling of Diesel Spray Combustion”, PhD Thesis, Chalmers University of Technology, 2001.
[35] Dukowicz, J.K., 1979. Quasi-Steady Droplet Change in the Presence Of Convection. Informal Report Los Alamos Scientific Laboratory, LA7997-MS.
[36] Hanjalic K, Popovac M, Hadziabdic M. A robust near-wall elliptic-relaxation eddy-viscosity turbulence model for CFD. Int J Heat Fluid Flow 2004; 25:1047–1051.
[37] Raju, M., Wang, M., Dai, M., Piggott, W. et al., "Acceleration of Detailed Chemical Kinetics Using Multi-zone Modeling for CFD in Internal Combustion Engine Simulations," SAE Technical Paper 2012-01-0135, 2012.

Acknowledgment

The authors gratefully acknowledge the financial support of the Interreg North-West Europe (Project No. NWE553). Additionally, the authors would like to thank the AVL Company for their collaboration in

this work to provide the AVL simulation software at YNCREA-HEI, France.

Nomenclature

ATDC	After Top Dead Center
BMEP	Brake Mean Effective Pressure
BDC	Bottom Dead Center
BSFC	Brake Specific Fuel Consumption
CA	Crank Angle
CA10, 50, 90	Crank angle at which 10%, 50%, 90% of total energy heat been released
CCS	Carbon Capture and Storage
CFD	Computational Fluid Dynamics
CO	Carbon monoxide
CO_2	Carbon dioxide
DI	Direct Ignition
EGR	Exhaust Gas Recirculation
H_2O	Water
HSDI	High Speed Direct Injection
HC	Hydrocarbon
HCCI	Homogenous Charge Compression Ignition
IC	Internal Combustion
IMEP	Indicated Mean Effective Pressure
ITE	Indicated Thermal Efficiency
IVC	Inlet Valve Closing
IVO	Inlet Valve Opening
LTC	Low temperature Combustion
NOx	Oxides of Nitrogen
O_2	Pure Oxygen
PM	Particulate Matter
RoHR	Rate of Heat Release
RPM	Revolutions per minute
SOI	Start of Injection
TDC	Top Dead Center
UHC	Unburned Hydrocarbons